Journal Name

ARTICLE TYPE

Cite this: DOI: 00.0000/xxxxxxxxxx

Hyperfine couplings between paramagnetic moment and nuclei in the metallic phase of low silica X zeolite loaded with potassium

Mutsuo Igarashi,*[a] Tadashi Shimizu,[b] Atsushi Goto,[b] Kenjiro Hashi,[b] Keiko Yamamichi,[a] and Takehito Nakano[c]

Received Date
Accepted Date

DOI: 00.0000/xxxxxxxxxx

Temperature dependences of NMR spectra have been observed for ^{23}Na and ^{27}Al in the metallic phase of Na-K form low silica X (LSX) zeolite loaded with potassium, where the condition of saturation is achieved with loading level of 9.0 atoms per supercage and the paramagnetic moment exists as contributing to the magnetism of the system beyond simple isolated spin. Separated two peaks have been recognized for ^{23}Na, where the shift values show quite linear relation with susceptibility and so-called K-χ plot works quite well to give values as 0.32 kOe/μ_B and 0.40 kOe/μ_B for hyperfine coupling constants. Although no separated peak is seen on ^{27}Al NMR spectrum, the spectral centroid deviates to positive side. The shoulder of the spectrum scales to susceptibility and K-χ plot also works well to give value as 0.15 kOe/μ_B for hyperfine coupling constant. Orbital of potassium-originated electron confined in the cage of LSX is understood as seeping out over the frame work of zeolite relatively wider than that of sodium-originated case.

1 Introduction

It is well known that alkali metal loading introduces metallic property into some kinds of zeolites[1]. Low silica X (LSX) is one of the representative zeolite substances on such the phenomenon. Metallic property of such the substrate with sodium loading has most extensively studied ever[2–4] than the one with other alkali species as potassium[5], rubidium[6], and so on. It has been known that the metallic phase of the system is accompanied with paramagnetic moment observed through susceptibility measurement and the appearance of separated component on ^{23}Na NMR spectrum[3,7,8] has been detected. Hyperfine coupling constant between such the paramagnetic moment and ^{23}Na has been estimated for sodium loading case through so called Clogston-Jaccarino plot[3]. On the other hand for ^{27}Al in this system, where only central component with temperature independent behavior on the NMR spectrum is observed, hyperfine coupling is at most takes quite less value than ^{23}Na[3]. It is concluded that orbital of the electron comes from loaded atoms is well confined within the cage of LSX in the case of sodium loading.

The skeletal structure type for LSX is FAU, which is the IUPAC nomenclature. When the system contains a monovalent cation M, the chemical formula is written as $M_{12}Al_{12}Si_{12}O_{48}$ per supercage (or β-cage). This corresponds to 1/8 of the cubic unit cell. We will refer to this as M-form LSX. Such a charge balance cation can be a complex one and the formula is rewritten as $Na_xK_{12-x}Al_{12}Si_{12}O_{48}$ for the case where both Na and K are included. We write it as Na_xK_{12-x}-LSX and refer to NaK-form LSX. x can vary from 0 to 12 by replacing the cation in aqueous solution.

Here we take a case of $x = 4$, where the formula is Na_4K_8-LSX. Na-K alloy clusters can be generated in its cages by loading guest K atoms. Following a previous report[9], we write the system as K_n/Na_4K_8-LSX. n is the number of loaded K atoms per supercage (or β cage). This system shows a ferrimagnetic transition for a narrow range of n around $n = 7.7$[10]. Spectra of ^{23}Na and ^{27}Al NMR have been observed for $n = 7.1$[7] where ferrimagnetic transition occurs at 7 K. It has a paramagnetic moment above 7 K, and several components have been detected that have shifts due to hyperfine interactions between the paramagnetic moment and ^{23}Na nuclei. As has been reported[5], this system shows metallic property for $n >\sim 6$. Studies with variation on n are expected to give hints to resolve the nature of the electron system. In this paper, we report NMR property of $n = 9.0$ case to explore how the behavior of such the component changes through increasing n.

2 Experimental

In the framework structure of LSX, β cages and supercages construct a double diamond structure[11]. Typical sites for cations

* E-mail: igarashi@gunma-ct.ac.jp
[a] National Institute of Technology, Gunma College, Maebashi, Gunma 371-8530, Japan.
[b] National Institute for Materials Science, Tsukuba, Ibaraki 305-0003, Japan.
[c] Institute of Quantum Beam Science, Graduate School of Science and Engineering, Ibaraki University, Mito, Ibaraki 310-8512, Japan.

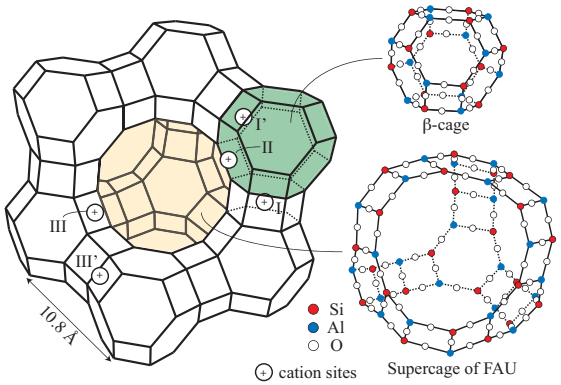

Fig. 1 Schematic illustration of the framework of low silica X zeolite. Possible cation sites based on symmetry are shown with small circles.

called site I, II and III are shown by small circles in Fig. 1. The sites for Al and Si atoms correspond to crossing points on the framework in the figure. The Si and Al atoms are alternatively ordered in the framework through the Si-O-Al bonds. Our sample is made of such the substance by loading of external K into those cages.

Sample preparation has been done with the same procedure as before[10]. Vapor of K atom is thermally absorbed in vacuum environment. The loading level was estimated as 9.0 K atoms per supercage using chemical analysis. Therefore the sample for the measurement is signed as $n = 9.0$. X-ray diffraction analysis has not been done for it but, taking into account the result of an analysis on the case of Na_n/Na_{12}-LSX[12], it is quite natural to consider that there are several kinds of sites for cations. No occurrence of magnetic transition has been detected with susceptibility measurement above 2 K, although previously reported sample of $n = 7.1$ shows ferrimagnetic transition at 7 K.

For NMR measurements, approximately 0.3 g of the powder sample was sealed in a quartz glass cell. The probe cell was cylindrical, with an outer diameter of 10 mm, an inner diameter of 8 mm, and an overall sample width of about 15 mm. NMR spectra of ^{23}Na and ^{27}Al have been measured at 63 kOe at several points of temperature below 300 K. References for the frequency shifts are taken with those of ^{23}Na and ^{27}Al in aqueous solution of NaCl and $AlCl_3$, respectively. Durations of first $(\pi/2)$ and second (π) pulse to obtain spin echo have typically been taken as 6 μs and 12 μs, respectively. Interpulse spacing for echo has typically been taken as 100 μs to obtain spin echo signal. NMR parameters for NMR measurement at representative temperatures are tabulated in Table 1. T_{1e} is an effective T_1 determined as a time that recovered magnetization becomes $1 - 1/e\,(\simeq 0.7)$ of thermal equilibrium one. It is estimated in the zero shift region of the spectrum, at where T_1 is relatively longer than tail part of the spectrum. Recycle delays between NMR measurements have been taken as sufficiently long to escape from saturation of the pulse excitation. However the case of 4 K, where magnetization recovery especially in the region close to zero shift has long time constant, violates such the constraint. Therefore quality of the data at 4 K is less than others. NMR spectrum is obtained by Fourier transformation of the spin echo signal. When the spectrum is wider than

Table 1 Measurement parameters for ^{23}Na NMR spectra.

Temperature (K)	Recycle delay (s)	Estimated T_{1e} (s)
300	2	< 0.1
90	20	~ 0.4
25	60	~ 0.7
4	60	-

Fourier component of the rf pulse, multiply obtained spectra at each frequency have been summed over for obtaining wide range spectrum. Susceptibility and optical spectra have been taken in the similar way in the reference[5].

3 Results and Discussion

3.1 ^{23}Na NMR

^{23}Na NMR spectrum of K_n/Na_4K_8-LSX at representative temperatures are shown in Fig. 2 for $n = 9.0$. Previously reported one for $n = 7.1$ are also shown[7]. In the region around zero shift the spectrum of this time data for $n = 9.0$ has a structured component similar to the one for $n = 7.1$.

In addition, a separated component labelled '#' accompanied with a somewhat large shift is seen at 300 K. The shift value of this component is ∼1400 ppm, which is different from that for ^{23}Na in the bulk metal sodium, ∼1100 ppm[13]. Such a sharp component with a large shift is not seen for $n = 7.1$. It was thought in the initial stage of the study that the component '#' was due to the metallic nature of the sample itself. But, the quite strange behavior of this component has changed such the recognition[8]. It disappears from the spectrum below between 220 K and 260 K through a complex hysteresis. It almost certainly comes from Na-K alloy distributed outside the particle of LSX crystal. Fortunately a contribution from it on the whole system is considered as quite minor. Based on signal intensity, the thickness of the Na-K alloy distributed on the surface of the zeolite crystal was estimated to be less than ∼ 30 nm, which is quite less than the average size of LSX crystal, ∼ 2 μm. Such a thin film can be assumed to have no influence on the optical spectra used to estimate the properties of the K clusters in the cages. In view of our aim, i.e. to discuss the properties of LSX with loaded K, we omit this separated component from the latter discussion.

In the structured component located in the center part, at least two shifted peaks are present. They are labeled P_1 and P_2, as shown in the inset of Fig. 2. The shifts of P_1 and P_2 become strong especially below 25 K. Accompanying such the behavior, width of the slopes in both side from the center part becomes large. Since we are interested in the shifts of the peaks, measurement has been omitted for negative shift side from the point at the symbol '*'. Even for P_1 and P_2 the location of them become ambiguous below 15 K. They are superimposed to the long tail in positive side.

Moreover, a weak but observable component with a temperature independent positive shift is observed, as indicated by '@' in the figure. The shift of this signal '@' has a shift of ∼ 1200 ppm.

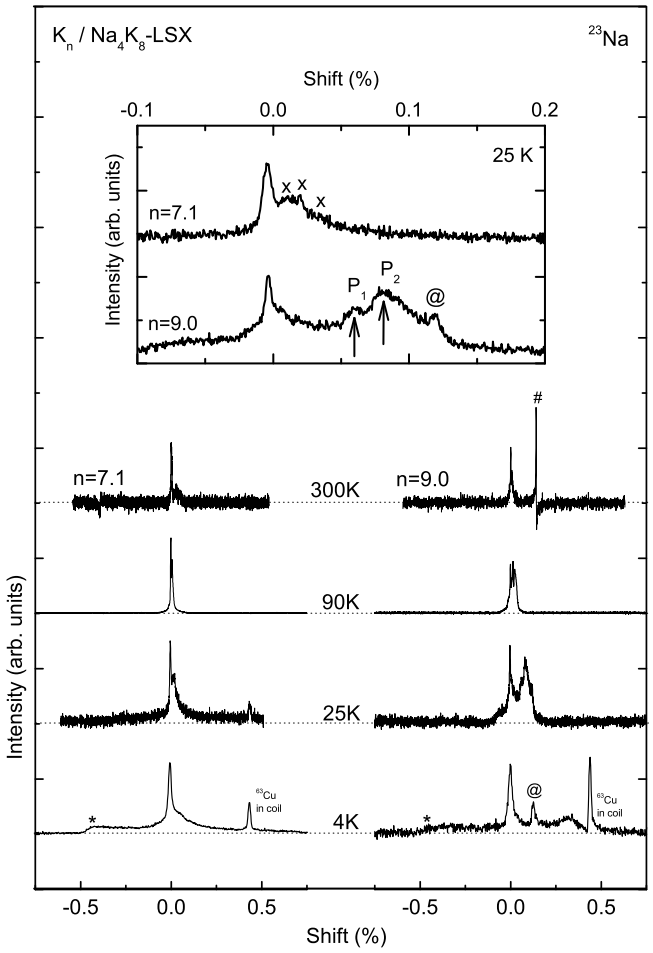

Fig. 2 ^{23}Na NMR spectra of K_n/Na_4K_8-LSX at representative temperatures in a field of 63 kOe for $n = 7.1$ and $n = 9.0$.

It is similar to that of ^{23}Na in the metallic bulk sodium[13]. For a similar reason as for the component labelled '#', we exclude it from the analysis. Although no additional experimental analysis was carried out for it, it could be a signal from deposited Na formed on the surface of the LSX crystal at the time of sample preparation.

We observed clear evidence on metallic property for the sample such as plasma edge on optical spectrum and expected temperature independent Knight shifts on NMR spectrum as an evidence for metallic nature. However, the shifts of the two peaks P_1 and P_2 depend on temperature. They can be manifestations of hyperfine coupling between the magnetic electrons and the nuclei via the Fermi contact interaction. Therefore, we need to confirm a relationship between Knight shift and susceptibility. The Knight shift is given by the non-zero probability of existence at the nuclear sites for electrons with the Fermi energy E_F. It is formally written as[14],

$$K = \frac{\Delta H}{H_0} = \frac{8\pi}{3} < |u_k(0)|^2 >_{E_F} \chi \equiv A\chi, \qquad (1)$$

where H_0 is the strength of the external magnetic field. ΔH is the deviation of the effective internal field from the external field at the nuclear site. Knight shift K is defined with both H_0 and ΔH. $u_k(0)$ is the wave function at the nuclear site and $< |u_k(0)|^2 >_{E_F}$ is an average of $|u_k(0)|^2$ at E_F. χ is the susceptibility of the electron system. A is the hyperfine coupling constant. In the case of a simple metal, χ is almost temperature independent and the Knight shift is essentially constant.

We made so called Clogston-Jaccarino plot (K-χ plot) to estimate A[15]. The peak positions have ambiguity on the spectra for lower temperatures as described above, the plot has been done above 15 K. It is shown in Fig. 3. Each data follows a straight line. Thus, we can evaluate A as the slope, K/χ, which are shown in the third column of Table 2. As instantly recognized, the component '@' is independent of χ. This is consistent with our assumption, where the component '@' comes from Na located outside of LSX crystals. Although K/χ is a dimensionless quantity in the CGS unit system†, the value of A is reported in many traditional papers with the unit Oe/μ_B, which allows us to compare the values between different substances. The unit Oe/μ_B means that we observe an effective field A Oe when a Bohr magneton $\mu_B = 9.27 \times 10^{-21}$ erg/Oe is located at the focused site. Then it is required to assume how much amount of the magnetic moment distributes at where it is. We are not currently able to rigorously estimate the distribution of the electron spins, some assumption must be included. In many cases of K_n/Na_xK_{12-x}-LSX, the Curie-Weiss law is observed in the temperature dependence of the magnetic susceptibility; the Curie constant is close to the value assuming a spin-1/2 localized magnetic moment in each β cage[1,5,9,10,16]. The ferrimagnetic and ferromagnetic orders observed at $0 \leq x \leq 4$ and $x \simeq 7$, respectively, at low temperatures cannot be explained without the presence of localized magnetic moments in β cages. Moreover, the presence of electrons confined in β cages is clearly observed in the optical spectra[16]. Therefore, we will estimate the value of the hyperfine coupling constant assuming a magnetic moment of one Bohr magneton per β cage. The cubic unit cell of this system with a lattice constant of 2.5 nm contains eight of β cages. Then one β cage corresponds to a volume $V_0 = 1.95 \times 10^{-21}$ cm^3. Then, A is given by $(K/\chi) \times (\mu_B/V_0)$ in the unit of Oe/μ_B. The obtained values are shown in the fourth column of Table 2. For ^{23}Na, P_1 and P_2 are thought to originate from two different crystallographic sites. A of P_1 is 80% of that of P_2. These values are directly proportional to the probability of the existence of electron spins on the nucleus at those sites, as is clear from eq. (1).

We attempted to fit the spectrum to characterize the three shift components, P_1, P_2 and '@'[17]. The fit results have two main characteristics: the P_2 component is three or more times broader than the other components, and the integrated intensity of the P_2 component is dominant, accounting for about 80% of the total, while those of P_1 and '@' are about 9% and 11%, respectively. Referring an analysis on the cation distribution for the hydrated Na_xK_{12-x}-

† K is clearly a dimensionless quantity by definition. χ is expressed in units of emu/cm^3 in this paper, which is also a dimensionless quantity in the CGS unit system.

Table 2 Values of K/χ by K-χ plot of the peaks on ^{23}Na and ^{27}Al NMR spectra.

Component Name	Nuclei	K/χ (cm^3/emu)	$(K/\chi)\times(\mu_B/V_0)$ (kOe/μ_B)
@	^{23}Na	1.6 ± 1.6	0.008 ± 0.008
P_1	^{23}Na	69 ± 2	0.33 ± 0.01
P_2	^{23}Na	86 ± 2	0.41 ± 0.01
D	^{27}Al	32 ± 3	0.15 ± 0.01

LSX by X-ray diffraction[18], the cation sites I and I' are most likely occupied by Na cations at $x=4$. As shown in Fig. 1, the site I is located at the center of doubled six-membered ring (D6R) and the site I' is located in the β cage on one side of D6R. Although the occupancy of Na cation sites in K-loaded samples is not completely known, we speculate the following from the NMR data. Since site I' is more inside the β cage than site I, we can expect a higher weight of the wave function of the electron confined in the β cage. Thus, P_2 with a larger A may originate from site I' and P_1 with a smaller A may originate from site I. This assumption is also supported by the spectral widths. Because ^{23}Na with $I=3/2$ has an electric quadrupole moment, the electric field gradient (EFG) dominates the spectral width. The site I in the center of D6R should have higher symmetry and have less EFG, resulting in the narrow spectrum. On the other hand, the site I' has a lower symmetry and has stronger EFG, resulting in the broader spectrum. As mentioned above, P_2 accounts for about 80% of the peak integrated intensity. This means that the occupancy of site I' is much higher than that of site I. It is quite possible that the distribution of Na cations in the dehydrated and K-loaded sample of K_n/Na_xK_{12-x}-LSX is different from that in the hydrated and non-loaded sample of Na_xK_{12-x}-LSX. Precise tracking of the variation of shifted peaks on NMR spectrum by changing the loading density is to be done to examine such occurrence. At lower temperatures, the spectrum becomes very broad due to the increase in paramagnetic magnetization of the electron spins. As seen in Fig. 2, the P_1 and/or P_2 component may be present around the 0.3% shift value at 4 K, but the peak positions are not clear, making analysis difficult. As mentioned earlier, the '@' component is independent of the bulk magnetic susceptibility. Therefore, it may originate from Na ions located on the surface or outside of the LSX crystal[8].

As seen in the inset of Fig. 2, there are several shifted peaks pointed with symbols of 'x' also for $n=7.1$. Although an analysis with K-χ plot has not yet been done for them, we are sure that those peaks also scales with χ. We gained a feeling that A seems to vary with n, although experiments with varying n has not been achieved yet. n variation of A may be one of a good index on electronic state in this system. We observed susceptibility of both $n=7.1$ and $n=9.0$ in the field of 63 kOe and obtained quite similar value. It is, for example, around 0.9×10^{-5} emu/cm^3 at 25 K. Increasing n makes effective local fields from such the similar magnitude of magnetic moment in the cage strengthen. Although K-χ plot has not ever been done for sample of $n=7.1$, A is expected to be smaller than $n=9.0$ case.

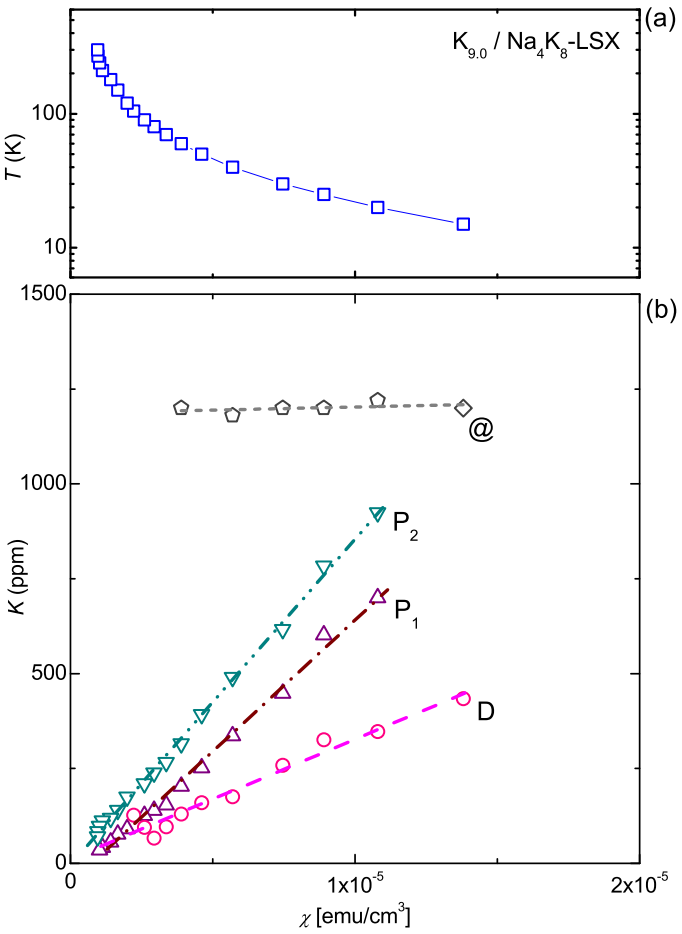

Fig. 3 Figures for the estimation of hyperfine coupling constants. (a) The susceptibility of $K_{9.0}/Na_4K_8$-LSX plotted versus temperature. (b) Clogston-Jaccarino plot (K-χ plot) of the shifts. Triangles with upper (purple) and lower (green) directions, labeled $^{23}P_1$ and $^{23}P_2$ in the figure, correspond to the peaks P_1 and P_2 on the ^{23}Na NMR spectra in the inset of Fig.2. Pentagons marked with the symbol '@' are also plotted in a similar manner. Open circles (red) are the shift values of the uppermost Gaussian component D in the four Gaussian fits for the shoulder of the ^{27}Al NMR spectrum in Fig.4. See text for the treatment of the curve fitting. Fitted to each data, the linear lines in (b) are drawn.

3.2 ^{27}Al NMR

The ^{27}Al spectrum of $n=9.0$ case at representative temperatures is shown in Fig. 4 together with the previously reported data of $n=7.1$[7]. The observation at 300 K for $n=9.0$ was not made because of its minor importance. Although there are spectral signals outside the area from the places marked with '*', we have omitted the observation of them by the similar reason. Based on our experience on various zeolites, the wider tailed area comes from satellite transition among Zeeman levels of ^{27}Al. The spin-spin relaxation time T_2 of such the transition is too short to give an observable spin echo signal at higher temperatures, but becomes slow at lower temperatures, allowing the spin echo signal to be observed. It is similar to a phenomenon reported for zeolite LTA[19], where T_2 of the satellite component tends to decrease by raising of temperature. Shortening T_2 causes a decrease in signal

intensity when observing the tailed components with constant τ, which is a separation time between rf pulses. Spectral width of the satellite powder pattern itself does not change with temperature. Since we are interested in the magnetic property and the mostly wider component can effectively be separated from the centered component around the peak, we omit the satellite components from our discussion.

Then we tried to fit the spectrum only for the centered component. As seen in the inset of Fig. 4, the higher shift side of the spectrum for $n = 9.0$ clearly has a shoulder-like structure at 25 K. The spectral centroid apparently has a positive shift. Since we still don't have precise knowledge on environment of nucleus and do not know appropriate functions to fit the experimental data, we tried to fit the whole spectrum with several Gaussians. At least four functions are needed to give a good coincidence. A typical example of the fitting result is shown in the inset of Fig. 4 by thin curves A, B, C and D located below the data points. Ratio of the integral intensity of the component D, $\frac{I_D}{I_A+I_B+I_C+I_D}$, is 3×10^1 %, where I_A, I_B, I_C and I_D are intensities of the components A, B, C and D, respectively.

A similar analysis worked well at lower temperatures, 4 K and 15 K[17]. The A and B components are understood to originate from the Al sites, where there is no Fermi contact with the electron wave function, since the spectral centroid does not change much with temperature. The spectral shape of the component whose centroid is shifted is not known analytically, but it can be reproduced by two components, C and D, when decomposed by the Gaussian function. These signals originate from Al sites with Fermi contact interactions with the electronic wavefunction.

As shown in Fig. 3(b), we created a K-χ plot for component D to evaluate the upper bound on the coupling constant. This plot fits quite well with a linear line. The hyperfine coupling constant has been estimated with the manner similar to the case of ^{23}Na and is also shown in Table 2. This non zero value means that the orbital of the electron confined in the cage seeps out from the cage into the site of ^{27}Al on the zeolite framework. The A of ^{27}Al is smaller than that of ^{23}Na. The probability of existence of the electron wave function on ^{27}Al is about 38–47% of that on ^{23}Na, estimated from the ratio of A.

Referring such the property, one notices little tilt on the higher shift side shoulder around the place marked with 'S' for the $n = 7.1$ sample as shown in the inset of Fig. 4. This may be a result of the shift caused by the hyperfine interaction. However, the shift is too small to estimate the coupling constant. Although it is difficult to discuss quantitatively, we can result that the difference of the shift is not given by difference of magnetic moment but is given by different coupling constant as is discussed above in the section of ^{23}Na. It is reasonable that higher loading of K into the cage leads the tail of the electron's orbital to seep out into the framework of LSX. It can also be said that the increase of the Fermi energy with the loading density causes a slight hybridization of the electronic states confined in the cage with those of the framework.

In Na-loaded sodalite, which is a type of zeolite, $A = 1.05$ kOe/μ_B was observed in the ^{27}Al NMR[20]. This value is much larger than that observed in this study in $K_{9.0}/Na_4K_8$-LSX. Sodalite has a much more compact crystal structure than LSX, with the β cages arranged in a body-centered cubic structure with a lattice constant of about 9 Å. The Na-loaded sodalite is an antiferromagnetic insulator with one unpaired s-electron occupying each cage. The high density of the structure is thought to cause a large overlap of the s-electron wavefunction with the Al position of the framework, resulting in a larger value of A compared to that in $K_{9.0}/Na_4K_8$-LSX.

4 Conclusion

^{23}Na and ^{27}Al NMR spectra between 300 K and 4 K of low silica X zeolite loaded with potassium for saturation level have been observed. For ^{23}Na, two peaks are found with susceptibility-scaled shift as similar to less-loaded sample, in which 7.1 potassium atoms are loaded per supercage. The magnitude of the shifts are several times larger than that of the less-loaded sample. The main cause is that the hyperfine coupling constants have become stronger. For ^{27}Al, a deformed spectrum is found with a shoulder-like shape on the higher frequency side of the peak, and the centroid of the entire spectrum has a temperature-variance-positive shift. The whole spectrum was analyzed with multiple sum of Gaussian functions, and the decomposed positively shifted component scales well with the susceptibility. The positively shifted component is concluded to be given by sites of ^{27}Al nuclei, which are located at the framework of zeolite, with hyperfine interaction from the atomic clusters in the cages. The less-loaded sample shows a symmetrically widened spectrum and gives at most quite little shift.

Author Contributions

M.I. designed the research. T.N. synthesized and characterized the sample. M.I., T.S., A.G., K.H., and K.Y. performed the NMR experiments. M.I. and K.Y. analyzed the NMR data. M.I. and T.N. wrote the main manuscript. M.I. finalized the manuscript. All authors reviewed the manuscript.

Conflicts of interest

There are no conflicts to declare.

Acknowledgements

The authors are grateful to Y. Nozue for his support. We also thank T. Kodaira and T. Ikeda for providing high-quality zeolite crystals, and S. Tamiya for the chemical analysis. This work was supported by JSPS KAKENHI (Grant Numbers JP15540353, JP15KK0165, JP16K05462, JP19K03738) and MEXT KAKENHI (Grant Number JP19051009).

Notes and references

1 T. Nakano and Y. Nozue, *Adv. Phys.: X*, 2017, **2**, 254–280.
2 T. Nakano, T. Mizukane and Y. Nozu, *J. Phys. Chem. Solids*, 2010, **71**, 650–653.
3 M. Igarashi, T. Nakano, P. T. Thi, Y. Nozue, A. Goto, K. Hashi, S. Ohki, T. Shimizu, A. Krajnc, P. Jeglič and D. Arčon, *Phys. Rev. B*, 2013, **87**, 075138–1–075138–7.
4 M. Igarashi, P. Jeglič, A. Krajnc, R. Žitko, T. Nakano, Y. Nozue and D. Arčon, *Sci. Rep.*, 2016, **6**, 18682–1–18682–8.

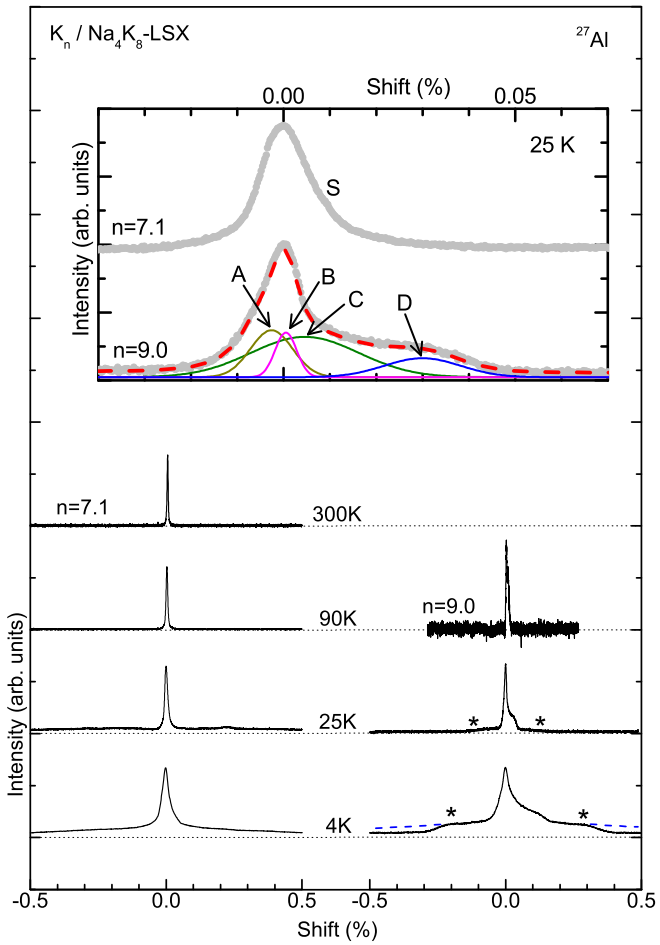

Fig. 4 ^{27}Al NMR spectra of K_n/Na_4K_8-LSX at representative temperatures in a field of 63 kOe for $n = 7.1$ and $n = 9.0$. The observation at 300 K for $n = 9.0$ was not made because of its minor importance. The Gaussian curves in the inset labeled A (brown), B (magenta), C (green), and D (blue) are extracted components by fitting the data, which corresponds to the thick-dashed line (red) on the experimental data (gray). The shift value of the peak of the component D is used in Fig.3 for the Clogston-Jaccarino plot. Measurements have been skipped for 25 K and 4 K on the spectral parts in the outer sides from the place signed with '*', because of less importance of them.

5 T. Nakano, D. T. Hanh, A. Owaki, Y. Nozue, N. H. Nam and S. Araki, *Journal of the Korean Physical Society*, 2013, **63**, 512–516.

6 P. Jeglič, T. Nakano, T. Mežnaršič, D. Arčon and M. Igarashi, *J. Phys. Soc. Jpn.*, 2020, **89**, 073706–1–073706–4.

7 M. Igarashi, T. Nakano, T. Shinizu, A. Goto, K. Hashi, K. Goto, K. Yamamichi and Y. Nozue, *J. Magn. Magn. Mater.*, 2007, **310**, e307–e309.

8 M. Igarashi, T. Shimizu, A. Goto, K. Hashi, K. Yamamichi and T. Nakano, *submitted*.

9 D. T. Hanh, T. Nakano and Y. Nozue, *J. Phys. Chemi. Solids*, 2010, **71**, 677–680.

10 T. Nakano, K. Goto, I. Watanabe, F. L. Pratt, Y. Ikemoto and Y. Nozue, *Physica B*, 2006, **374–375**, 21–25.

11 H. A. M. Verhulst, W. J. J. Welters, G. Vorbeck, L. J. M. van de Ven, V. H. J. de Beer, R. A. van Santen and J. W. de Haan, *J. Phys. Chem.*, 1994, **98**, 7056–7062.

12 T. Ikeda, T. Nakano and Y. Nozue, *J. Phys. Chem. C*, 2014, **118**, 23202–23211.

13 *Metallic Shifts in NMR*, ed. G. C. Carter, L. H. Bennett and D. J. Kahan, Pergamon Press, Oxford, 1977.

14 C. P. Slichter, *Principles of Magnetic Resonance*, Springer-Verlag, Berlin, 1989.

15 A. M. Clogston, V. Jaccarino and Y. Yafet, *Phys. Rev.*, 1964, **134**, A650–A661.

16 L. M. Kien, T. Goto, D. T. Hanh, T. Nakano and Y. Nozue, *J. Phys. Soc. Jpn.*, 2015, **84**, 064718–1–064718–9.

17 See Electric Supplementary Information.

18 Y. Lee, S. W. Carr and J. B. Parise, *Chem. Mater.*, 1998, **10**, 2561–2570.

19 M. Igarashi, T. Kodaira, T. Shimizu, A. Goto, K. Hashi, T. Nakano and Y. Nozue, *Chem. Phys. Lett.*, 2007, **436**, 80–83.

20 I. Heinmaa, S. Vija and E. Lippmaa, *Chemical Physics Letters*, 2000, **327**, 131–136.